Electronic Supplementary Material (ESI) for Journal of Materials Chemistry A.

Supporting Information for

Electrochemical Supercapacitor with Polymeric Active Electrolyte

Libin Chen, Yanru Chen, Jifeng Wu, Jianwei Wang, Hua Bai*, and Lei Li*

College of Materials, Xiamen University, Xiamen, 361005, P. R. China.

E-mail: baihua@xmu.edu.cn; lilei@xmu.edu.cn

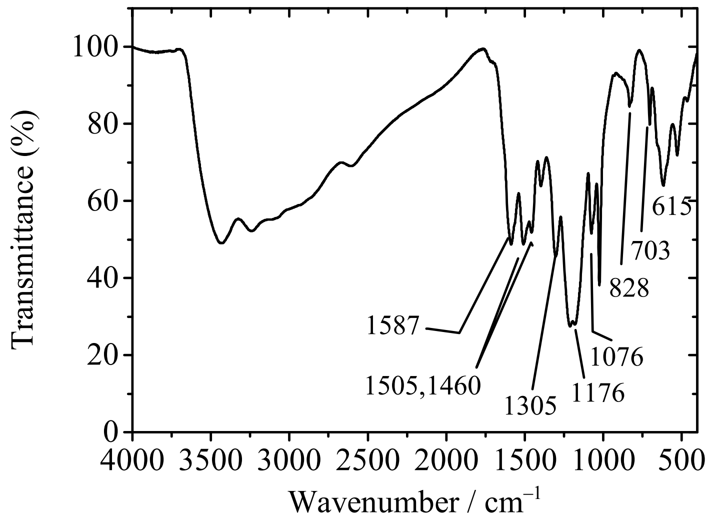

Fig. S1 IR spectrum of SPAni.

As shown in Fig. S1, the absorption bands at 1587 and 1305 cm^{-1} are ascribed to the C=N stretching vibration and C−N bending vibration of SPAni backbone. The absorption at 1505, 1460 cm^{-1} can be ascribed to the C=C stretching vibration of benzene ring, and the absorption bands at 828 cm^{-1} are corresponding to the bending vibration of CH on 1,2,4-trisubstituted benzene rings. The characterristic absorption band of O=S=O asymmetric and symmetric stretching vibration are centered at 1176 and 1076 cm^{-1}. Peaks at 703 and 615 cm^{-1} are assigned to S−O and C−S stretching vibrations, respectively [1]. According to the IR of the polymer, polyaniline was successfully sulfonated.

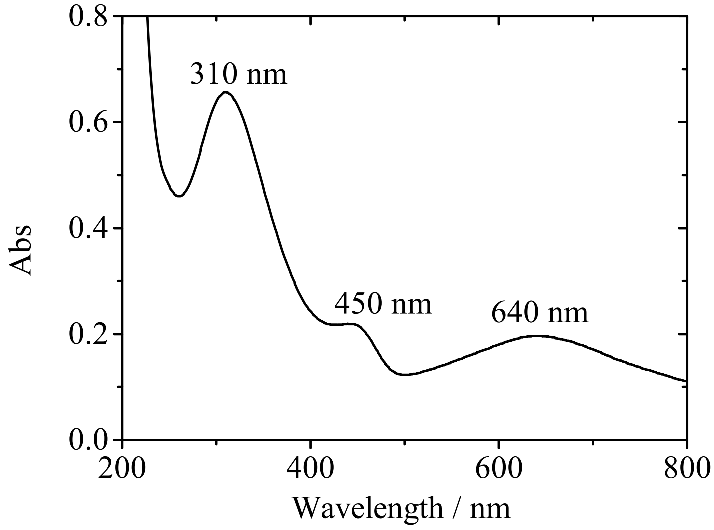

Fig. S2 The UV-Vis spectrum of SPAni.

The absorption peak at 310 nm is ascribed to the π-π electron transition of benzene ring, the absorption at 450 nm is the polaron band. The wide band around 640 nm can be ascribed to the undoped quinoid units [1].

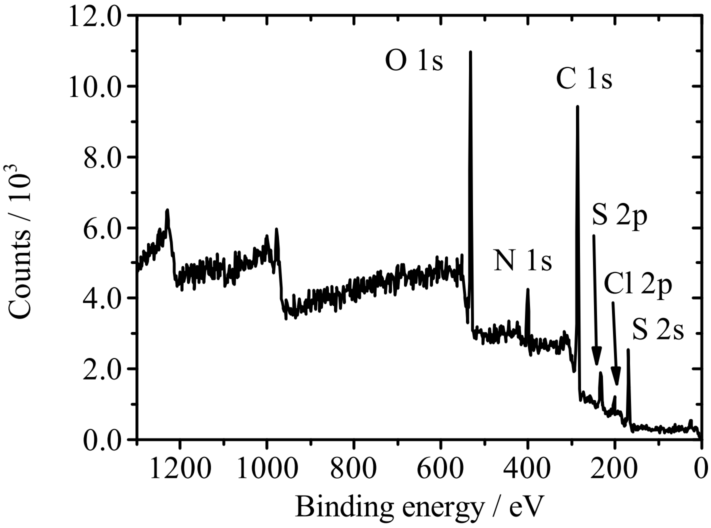

Fig. S3 XPS of SPAni.

S/N ratio measured by XPS is 0.65:1. Therefore, about 65% benzene rings in the backbone of SPAni were sulfonated.

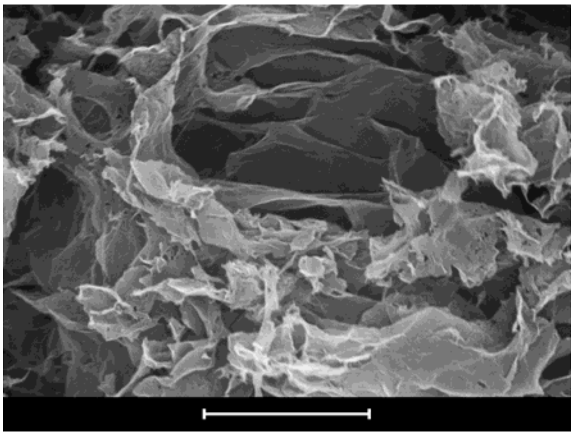

Fig. S4 SEM image of as prepared GHG, showing porous structure composed of loosely packed GHG sheets.

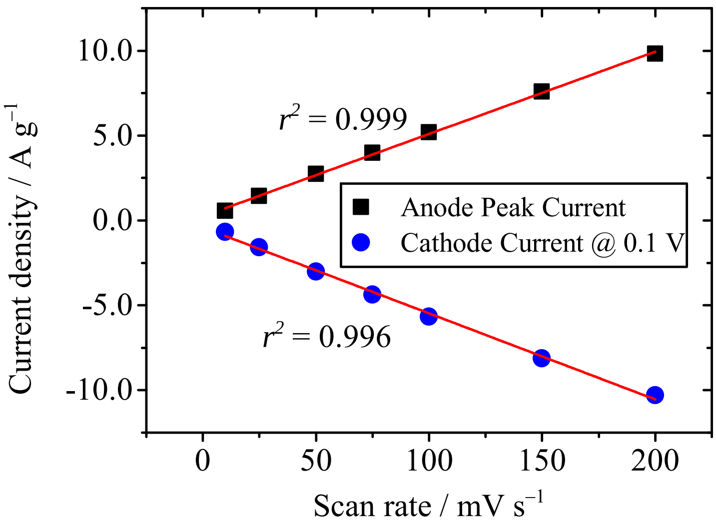

Fig. S5 Plot of current density versus scan rate in CV curves of Device 1.

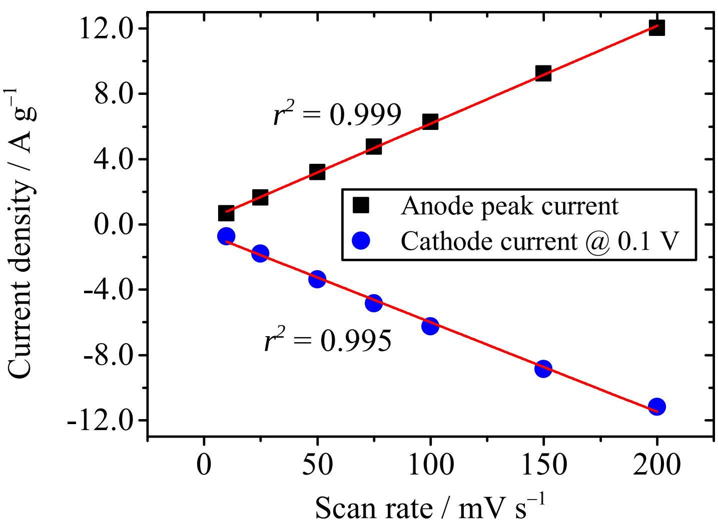

Fig. S6 Plot of current density versus scan rate in CV curves of Device 2.

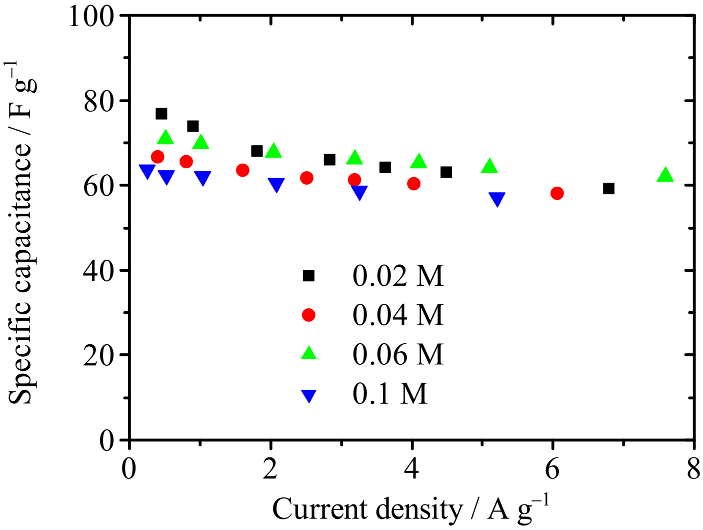

Fig. S7 Specific capacitances of devices at different concentration of SPAni between 0.02 M and 0.1 M.

From Fig. S7 it can be seen that, at different current densities, the specific capacitances of different devices are within the range of 60 ~ 70 F g^{-1}. We did not find obvious regular pattern from these data, thus the concentration of SPAni has little effect on the specific capacitance of the device. The deviation between these data is caused by slightly different mass ratio of two electrodes in different devices. This result demonstrated that SPAni in above concentration range is enough for energy store in Device 2.

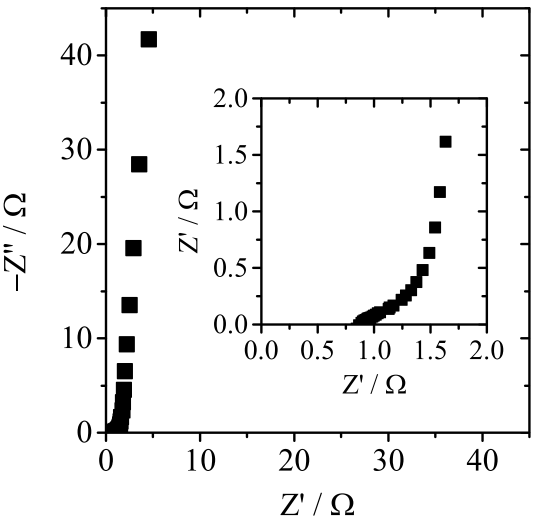

Fig. S8 Nyquist plots of Device 2. Inset: magnified high-frequency regions.

The Nyquist plot of the Device 2 starts with a 45º region (Warburg region), which can be attributed to diffusion of electrolyte in the porous GHG electrode. At low frequencies, the straight line is nearly perpendicular to the real axis, indicating the purely capacitive behavior of the device. The equivalent series resistance of Device 2 was measured to be about 1.5 Ω by extrapolating the straight line to intersect the real axis.

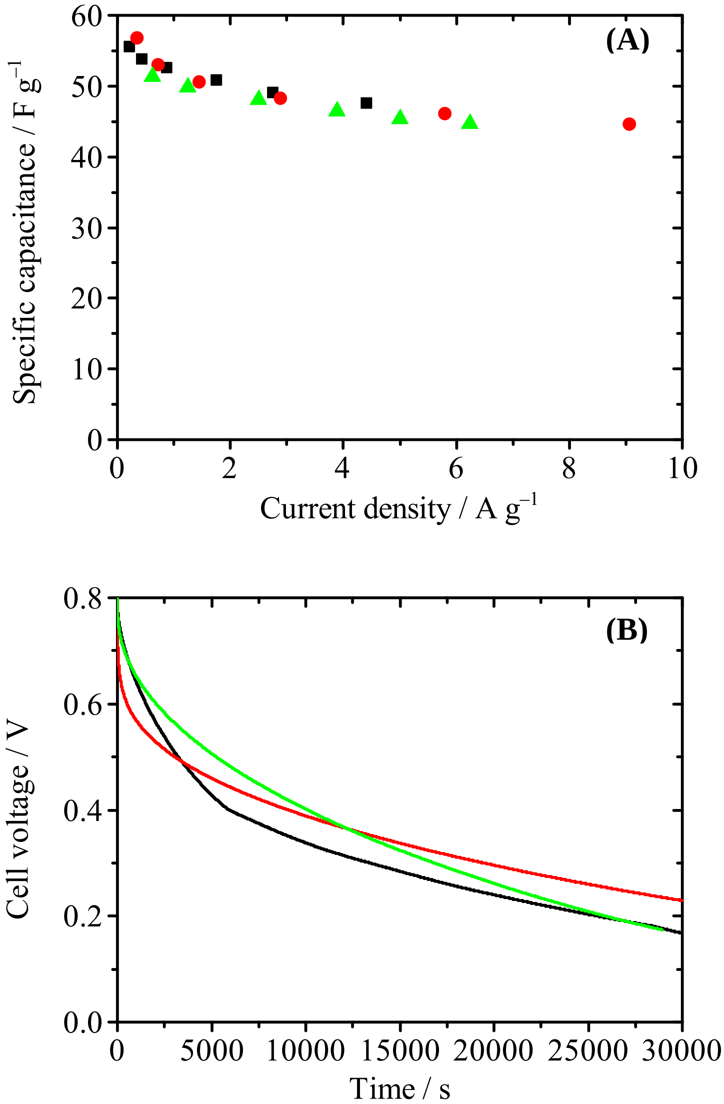

Fig. S9 Repeatability of Device 1. (A) Specific capacitance of three individual devices. (B) Self-discharge curves of three individual devices.

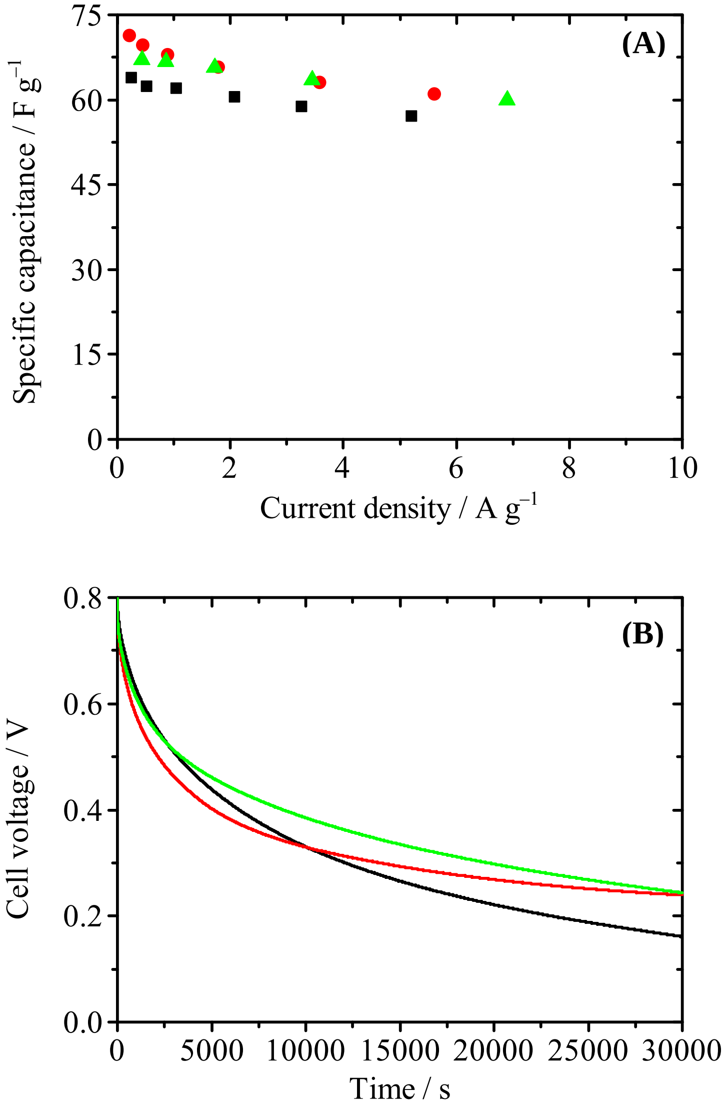

Fig. S10 Repeatability of Device 2. (A) Specific capacitance of three individual devices. (B) Self-discharge curves of three individual devices.

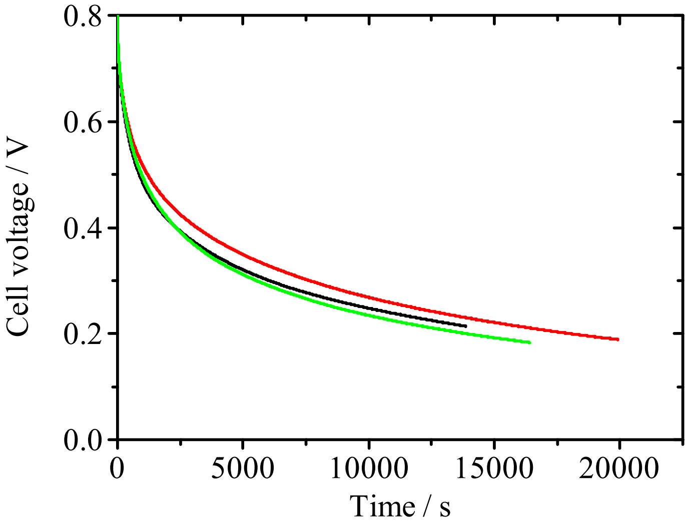

Fig. S11 Self-discharge curves of three individual devices.

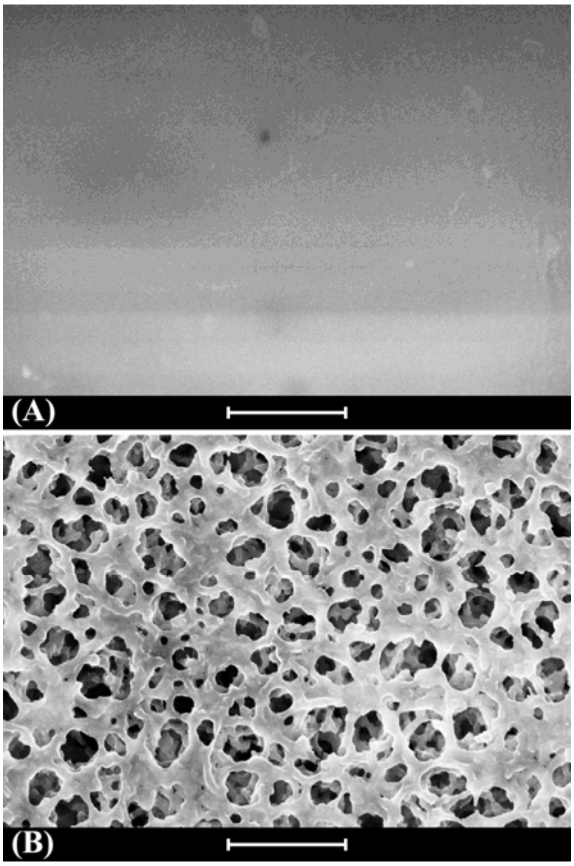

Fig. S12 The SEM image of (A) dialysis tube and (B) cellulose acetate membrane. Scale bar: 2 μm.

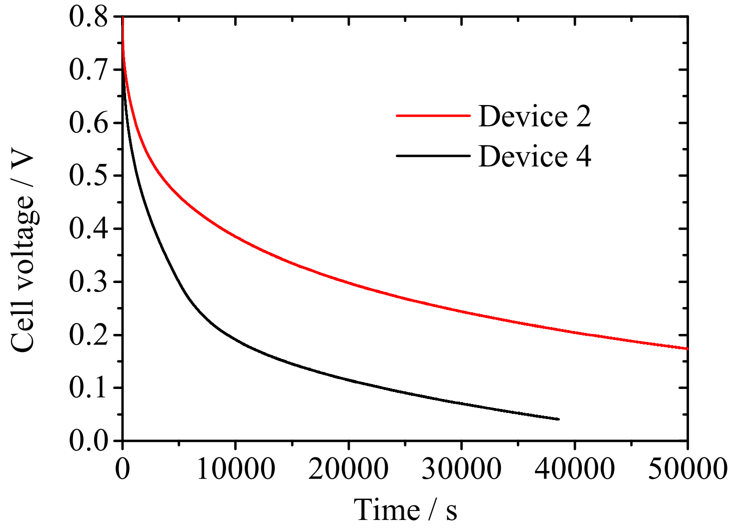

Fig. S13 Self-discharge curves of Device 2 (0.1 M SPAni + 4 M H_2SO_4, with semipermeable membrane as separator) and Device 4 (0.1 M HQ + 4 M H_2SO_4, with semipermeable membrane as separator).

Reference

[1] S. Ito, K. Murata, S. Teshima, R. Aizawa, Y. Asako, K. Takahashi, B. M. Hoffman, *Synth. Met.,* 1998, **96**, 161−163.